

F.I. Parra, M.F.F. Nave, A.A. Schekochihin, C. Giroud, J.S. de Grassie,
J.H.F. Severo, P. de Vries, K.-D. Zastrow and JET EFDA contributors

Scaling of Spontaneous Rotation with Temperature and Plasma Current in Tokamaks

“This document is intended for publication in the open literature. It is made available on the understanding that it may not be further circulated and extracts or references may not be published prior to publication of the original when applicable, or without the consent of the Publications Officer, EFDA, Culham Science Centre, Abingdon, Oxon, OX14 3DB, UK.”

“Enquiries about Copyright and reproduction should be addressed to the Publications Officer, EFDA, Culham Science Centre, Abingdon, Oxon, OX14 3DB, UK.”

The contents of this preprint and all other JET EFDA Preprints and Conference Papers are available to view online free at www.iop.org/Jet. This site has full search facilities and e-mail alert options. The diagrams contained within the PDFs on this site are hyperlinked from the year 1996 onwards.

Scaling of Spontaneous Rotation with Temperature and Plasma Current in Tokamaks

F.I. Parra^{1,2}, M.F.F. Nave^{3,1}, A.A. Schekochihin¹, C. Giroud⁴, J.S. de Grassie⁵, J.H.F. Severo⁶, P. de Vries⁷, K.-D. Zastrow⁴ and JET EFDA contributors*

JET-EFDA, Culham Science Centre, OX14 3DB, Abingdon, UK

¹*Rudolf Peierls Centre for Theoretical Physics, University of Oxford, Oxford OX1 3NP, UK*

²*Plasma Science and Fusion Center, Massachusetts Institute of Technology, Cambridge, MA 02139, USA*

³*Associação EURATOM/IST, Instituto de Plasmas e Fusão Nuclear-Laboratório Associado, Lisbon, Portugal*

⁴*EURATOM-CCFE Fusion Association, Culham Science Centre, OX14 3DB, Abingdon, OXON, UK*

⁵*General Atomics, P.O. Box 85608, San Diego, California, USA*

⁶*Institute of Physics, University of São Paulo, SP, Brazil*

⁷*FOM Institute for Plasma Physics, Rijnhuizen, Association EURATOM-FOM, Nieuwegein, The Netherlands*

** See annex of F. Romanelli et al, "Overview of JET Results", (23rd IAEA Fusion Energy Conference, Daejeon, Republic of Korea (2010)).*

ABSTRACT.

A simple law for the size of the intrinsic rotation observed in tokamaks in the absence of momentum injection is found: the velocity in the counter-current direction generated in the core of a tokamak is proportional to the ion temperature difference in the core divided by the plasma current, independent of the size of the device. The constant of proportionality is of the order of $10\text{km}\cdot\text{s}^{-1}\cdot\text{MA}\cdot\text{keV}^{-1}$. This law is derived using theoretical arguments and confirmed experimentally for several tokamaks of different size and heated by different mechanisms.

1. INTRODUCTION

Due to their axisymmetry, tokamak plasmas can be made to rotate at high speeds if momentum is injected into them. If the rotation shear is sufficiently large, large scale MagnetoHydroDynamic (MHD) instabilities are stabilized [1] and the turbulent transport of energy can be much reduced [2–4]. Unfortunately, ITER [5], the largest magnetic confinement experiment currently being built, is not expected to have effective momentum deposition due to its size and high density. As a result, there has been mounting interest in the intrinsic, or spontaneous, rotation observed in tokamaks without momentum injection [6]. If this intrinsic rotation could be made large, it could be used to reduce turbulence as is done with momentum injection. Understanding the origin of this rotation is also an interesting physics question in itself. In this Letter, we use very simple theoretical arguments to show that the velocity difference within the core of a tokamak must scale proportionally to the ion temperature difference divided by the plasma current. The constant of proportionality is independent of machine size and is of order $c^2/e = 10\text{km}\cdot\text{s}^{-1}\cdot\text{MA}\cdot\text{keV}^{-1}$, where c is the speed of light and e is the proton charge. By comparing experimental data from machines whose sizes range from tens of centimeters to several meters, that have very different plasma currents (from 0.1MA to 2.5MA), and that are heated by different mechanisms (JET [7], DIII-D [8], TCABR [9] and TCV [10]), we show that the intrinsic rotation in the counter-current direction follows the theoretical scaling.

2. THEORETICAL ARGUMENTS

In a tokamak plasma, turbulence and collisions transport particles, energy and momentum across magnetic surfaces. The energy losses are compensated by external heating. Particles can be injected via pellets of frozen gas, but most come from gas fuelling and wall recycling at the edge. Momentum can be injected with neutral beams and even with Radio Frequency waves (RF) [11], but in many occasions there is no external source of momentum. When the latter is the case, the toroidal angular momentum flux through every flux surface must be zero, even though significant rotation can often be observed experimentally. Only the angular momentum in the toroidal direction is relevant. In the poloidal direction, the flow is strongly damped by collisional processes, which pass the momentum through the magnets to the structure of the tokamak. Thus, to calculate the profile of spontaneous rotation, it is necessary to calculate the dependence of Π on the toroidal rotation frequency Ω_ϕ and then solve the equation $\Pi(\Omega_\phi) = 0$ for Ω_ϕ .

Both turbulence and collisions occur on time scales that are longer than the inverse of the

gyrofrequency, which means that the particle trajectories can be understood as a fast gyromotion around guiding centres, which move fast along magnetic field lines and drift slowly across them. This is the physical idea underlying gyrokinetics, which is the most commonly used approximation in transport simulations [12–16].

Even in the absence of turbulence and collisions, particles move out of the surface of constant magnetic flux where they started due to the ∇B and curvature drifts, but they remain within a given distance of it. This distance is approximately given by the poloidal gyroradius $\rho_\theta = mc v_{th} / e B_\theta$, where e and m are the charge and mass of the particle, v_{th} is the thermal speed, and B_θ is the poloidal component of the magnetic field. Note that $\rho_\theta = (B/B_\theta)\rho$, where ρ is the particle gyroradius and B is the total magnetic field. In most tokamaks, B/B_θ is of order 10. Tokamaks are constructed so that $\rho_\theta \ll L_T$, where L_T is the characteristic length of variation of the temperature L_T , which we use as our length of reference.

Collisions cause transport, known as neoclassical transport [17], because each collision makes the particle move from one drift orbit to another drift orbit separated by ρ_θ . Because $\rho_\theta/L_T \ll 1$, it takes many collisions for the particles to travel from the high temperature to the low temperature region, and the transport is diffusive.

Turbulent transport is caused by electromagnetic fluctuations, of which the most virulent are believed to be driven by the Ion Temperature Gradient (ITG). The perpendicular characteristic size of ITG turbulence structures scales as $(B/B_\theta)(a/L_T)\rho \sim \rho_\theta$, where a is the minor radius of the tokamak ($L_T \sim a$). This scaling is not based on the drift orbits as is in the case of collisional transport, but on critical balance between the parallel and the perpendicular dynamics [18]. Not every type of turbulence scales like this, but we believe that this is the maximum perpendicular scale than can be achieved in most experimental situations.

In general, tokamaks are geometrically up-down symmetric to a great degree in the core. In such tokamaks, to lowest order in ρ_θ/L_T , the transport of momentum can only be different from zero if a preferred direction is given by either rotation or rotational shear [19]. Here we are assuming $\Omega_\phi \sim v_{th}/R$, this being the ordering for which the rotation and its shear enter in the lowest order gyrokinetic equation [20, 21]. The direction of the magnetic field is not sufficient to break the up-down symmetry. Thus, schematically, to lowest order in ρ_θ/L_T ,

$$\Pi \sim -v_t R^2 \left(\frac{\partial \Omega_\phi}{\partial r} + \frac{\Omega_\phi}{\ell_{pinch}} \right) - v_c R^2 \frac{\partial \Omega_\phi}{\partial r}, \quad (1)$$

where r is the radial coordinate, R is the major radius, v_t is the turbulent viscosity, v_t/ℓ_{pinch} is the turbulent pinch of momentum [22, 23], and v_c is the collisional viscosity.

The equation for intrinsic rotation is $\Pi = 0$, and with the lowest-order expression (1) for Π , the solution is $\Omega_\phi \propto \exp(-\int dr/\ell_{pinch})$. It is then possible to obtain intrinsic rotation if rotation is generated in some region of the plasma (for example, in the edge) and pinched to other regions. However, this mechanism is not fully satisfactory because it cannot explain the variety of observed profiles [7]. In particular, Ω_ϕ cannot change sign, contradicting experimental observations (as we will show in the

next section). Unfortunately, to lowest order, Eq. (1) is correct and no other mechanism for intrinsic rotation can be obtained.

If the expansion in $\rho_\theta/L_T \ll 1$ is continued to next order, the rotation and its shear are not the only physical factors that provide a preferred direction and can give raise to momentum transport: the pressure and temperature gradients also break the up-down symmetry by, for example, making the plasma rotate poloidally. Consider the guiding centres of two particles (1 and 2) that at point some point A at the outboard midplane of a tokamak have velocities in opposite directions, as sketched in Fig.1. The dashed line represents the cut of a surface of constant magnetic flux through a poloidal plane (the axis of symmetry is the dash-dot line). The poloidal magnetic field B_θ is parallel to the dashed line and points counterclockwise, whereas the toroidal magnetic field B_ϕ points towards the reader. At point A, particle 1 (red orbit) travels counterclockwise, and since to lowest order it follows the magnetic field, its toroidal velocity $v_{\phi 1}$ is pointing towards the reader. Particle 2 (blue orbit) travels in the opposite direction both poloidally and toroidally. Orbits do not follow the flux surface exactly, but separate from it a small distance of order ρ_θ . Particle 1 moves towards the center of the tokamak due to the ∇B and curvature drift because its poloidal orbit is counterclockwise. Particle 2 drifts outwards. Because of the temperature gradient, the center of the tokamak is hotter, and particles like particle 1 will have more energy, of the order of $(\rho_\theta/L_T)mv_{th}^2$, breaking the symmetry and, in this simplified picture, making the plasma rotate counterclockwise poloidally, and towards the reader toroidally. Figure 1 shows that whereas the direction of the magnetic field is unimportant, the vector $\mathbf{B} \times \nabla T$ does give a preferred direction at higher order in ρ_θ/L_T parallel to or against which the plasma will tend to rotate. The mechanism described here does not determine the sense of the toroidal rotation, but it does demonstrate that background gradients break the up-down symmetry and that the effects of this symmetry breaking are of order ρ_θ/L_T . Calculating all these effects is a rather sophisticated analytical task, involving many factors subtler than the simple argument given above.

The next-order collisional contributions to momentum transport in $\rho_\theta/L_T \ll 1$ were first calculated in neoclassical theory [24, 25], where they are proportional to radial derivatives of the ion temperature. Models to calculate the next-order contributions to turbulent transport have also been proposed [26, 27]. In general, we expect the new next-order terms to depend strongly on density and temperature gradients because these drive the turbulence. Schematically, as shown in [26], we may write

$$\begin{aligned} \Pi \sim & -v_t R^2 \left[\frac{\partial \Omega_\phi}{\partial r} + \frac{\Omega_\phi}{\ell_{pinch}} + O \left(\frac{\rho_\theta}{L_T} \frac{v_{th}}{RL_T} \right) \right] \\ & - v_c R^2 \left[\frac{\partial \Omega_\phi}{\partial r} + O \left(\frac{\rho_\theta}{L_T} \frac{v_{th}}{RL_T} \right) \right]. \end{aligned} \quad (2)$$

From (2), setting $\Pi = 0$ and assuming that the scale length of Ω_ϕ is of order L_T , we obtain $R\Omega_\phi \sim (\rho_\theta/L_T)v_{th} \sim (c/eB_\theta)(T/L_T)$, where $T = mv_{th}^2/2$ is the temperature. The poloidal magnetic

field is given by the toroidal plasma current I_p , $B_\theta \sim 4 I_p / c L_B$, where L_B is the characteristic length of variation of B_θ . Therefore, $R\Omega_\phi \sim (L^B/L_T)(c^2/e)(T/I_p)$. In the core, L_B and L_T are both of the order of the minor radius a , so the toroidal velocity is

$$V_\phi = R\Omega_\phi \sim \frac{c^2}{e} \frac{T}{I_p}. \quad (3)$$

This equation gives a strong constraint on the intrinsic rotation in the core in terms of the temperature and the plasma current, but independently of machine size. The dimensional constant of proportionality is $c^2/e = 10 \text{ km} \cdot \text{s}^{-1} \cdot \text{MA} \cdot \text{keV}^{-1}$.

3. EXPERIMENTAL MEASUREMENTS

We now compare experimental data from different machines that show similarities in their intrinsic rotation profiles. In Fig.2, we show two pulses from JET that represent two distinct types of intrinsic rotation profiles: the ones in which the toroidal velocity increases from the magnetic axis towards the edge of the tokamak (red profile), which we call hollow profiles, and the ones in which it decreases (blue profile), which we call peaked profiles (the toroidal velocity is deemed positive if it is co-current). The two pulses in Fig.2 have very different input power and plasma current, and they are only meant to be examples of the two types of velocity profiles. The peaked profiles need not have higher temperature gradients than the hollow profiles. The velocity at the edge is mostly co-current, and this seems to be common to all tokamaks with low magnetic ripple in the absence of momentum injection. In JET, the hollow profiles correspond to Ohmic shots and some of the Ion Cyclotron Resonance Heating (ICRH) pulses in both Low-Confinement Mode (L-mode) [7] and High-Confinement Mode (H-mode) [28]. The cases with peaked profiles are all ICRH L-mode and H-mode shots.

To check (3), we compare the pulses with hollow core velocity profile for four different tokamaks: JET [7], DIII-D [8], TCABR [9] and TCV [10]. To characterize the velocity generated intrinsically in the core, we use the difference in toroidal velocity ΔV_ϕ between the minimum of toroidal velocity closest to the magnetic axis on the outboard side and the first maximum encountered when moving from the magnetic axis towards the edge on the outboard side. This definition of ΔV_ϕ is illustrated in Fig.2(a). The parameter ΔV_ϕ attempts to exclude any intrinsic velocity generated at the edge – most likely by means not covered in our theoretical discussion above. To give a measure of the sources generating intrinsic rotation in (2), we use the difference in ion temperature ΔT_i between the magnetic axis and the temperature at the top of the pedestal in H-modes, or the temperature at the separatrix in L-modes. This measure, illustrated in Fig.2(b), excludes the ion temperature jump in the pedestal in the case of H-modes. In Fig.3, we show $I_p \Delta V_\phi$ versus T_i for various tokamaks [?]. According to (3), we expect

$$I_p \Delta V_\phi = \alpha \frac{c^2}{e} \Delta T_i. \quad (4)$$

The dimensionless prefactor α could not be determined in our qualitative theoretical discussion,

but we can find its value from the present experimental analysis. The data is consistent with an approximate linear dependence with a slope of $(18\pm 4)\text{km}\cdot\text{s}^{-1}\cdot\text{MA}\cdot\text{keV}^{-1}$ for all machines, giving $\alpha \simeq 1.8\pm 0.4$. The slope was determined by least-square fitting and the error is the 99% confidence interval. Note that in Fig.3 there are Ohmic, ICRH and Electron Cyclotron Resonance Heating (ECRH) shots, Land H-modes, plasma currents spanning from 0.1MA to 2.5MA, and machines of sizes ranging from tens of centimeters (TCABR) to meters (JET). The fact that both the scaling and the prefactor seem to be valid for this variety of situations suggests that the theoretical ideas proposed above are robust.

However, when the same analysis was attempted for the peaked proles in JET, the trend was not so clear. There are several possible explanations. In [29, 30], a change from Trapped Electron Mode (TEM) driven turbulence to ITG turbulence was proposed as the cause for the transition between hollow and peaked proles. If this is the case, it is possible that T_i is not a good parameter to work with because it does not contain information about the electrons. It is also possible that the peaked-prole cases are dominated by the inward pinch of momentum generated at the edge [7], making the rotation in the core correlated to the parameters at the edge and not to the parameters of the core. Note that even though the trend with ΔT_i and I_p was not so clear, the velocity difference ΔV_ϕ was still of the same order as (3).

DISCUSSION

Using simple theoretical arguments and data from several tokamaks, we have shown that the intrinsic rotation in the counter-current direction in the core scales according to (4).

There are ways of generating intrinsic rotation that have not been considered in this Letter. For example, in the core, RF heating can transport momentum within the core [31, 32] due to large orbits of energetic ions. In the edge, direct particle losses can generate rotation. It seems that these effects are not important in the cases presented in Fig.3 because these include shots with and without energetic ions, and with and without a pedestal. We do not know how generic this is. We have introduced a dimensionless parameter $\alpha = eI_p\Delta V_\phi/c^2\Delta T_i$, which was of order unity for a variety of regimes and machines considered here. It would be very instructive to quantify experimentally measured rotation in other cases in terms of this parameter. In cases that α is significantly larger than unity, the rotation must have external origin, such as energetic ions, edge effects or momentum injection. The experimental results presented above cannot determine if the transport of momentum is dominated by collisions or turbulence because both have the same scaling (3). Since turbulent viscosity is of the same order as the thermal diffusivity [23, 32, 34, 35], and turbulent transport usually dominates, we expect the ρ_ϕ/L_T corrections to the turbulent momentum transport to play the dominant role in driving intrinsic rotation.

ACKNOWLEDGEMENTS

The authors acknowledge many helpful discussions with M. Barnes and T. Johnson. This work was supported in part by EPSRC, STFC, the Leverhulme Trust Network for Magnetized Plasma

Turbulence, the US DOE under DE-FC02-04ER54698, the European Communities through Association Euratom/IST, and carried out within the frameworks of the Instituto de Plasmas e Fusão Nuclear-Laboratório Associado and the European Fusion Development Agreement. It received financial support from Fundação para a Ciência e Tecnologia (FCT), Portugal. The views and opinions expressed herein do not necessarily reflect those of the European Commission.

REFERENCES

- [1]. A. Bondeson and H. X. Xie, *Physics of Plasmas* **4**, 2081 (1997).
- [2]. J.W. Connor et al., *Nuclear Fusion* **44**, R1 (2004).
- [3]. P.C. de Vries et al., *Nuclear Fusion* **49**, 075007 (2009).
- [4]. P. Mantica et al., *Physical Review Letters* **102**, 175002 (2010).
- [5]. K. Ikeda et al., *Nuclear Fusion* **47**, E01 (2007).
- [6]. J.E. Rice et al., *Nuclear Fusion* **47**, 1618 (2007).
- [7]. L.-G. Eriksson et al., *Plasma Physics and Controlled Fusion* **51**, 044008 (2009).
- [8]. J.S. deGrassie et al., *Physics of Plasmas* **14**, 056115 (2007).
- [9]. J.H.F. Severo et al., *Nuclear Fusion* **43**, 1047 (2003).
- [10]. A. Scarabosio et al., *Plasma Physics and Controlled Fusion* **48**, 663 (2006).
- [11]. A. Ince-Cushman et al., *Physical Review Letters* **102**, 035002 (2009).
- [12]. W. Dorland et al., *Physical Review Letters* **85**, 5579 (2000).
- [13]. J. Candy and R.E. Waltz, *Journal of Computational Physics* **186**, 545 (2003).
- [14]. T. Dannert and F. Jenko, *Physics of Plasmas* **12**, 072309 (2005).
- [15]. A.G. Peeters et al., *Computer Physics Communication* **180**, 2650 (2009).
- [16]. M. Barnes et al., *Physics of Plasmas* **17**, 056109 (2010).
- [17]. F. L. Hinton and R.D. Hazeltine, *Review of Modern Physics* **48**, 239 (1976).
- [18]. M. Barnes, F.I. Parra and A.A. Schekochihin, submitted to *Physics of Plasmas* arXiv:1104.4514.
- [19]. F.I. Parra, M. Barnes and A.G. Peeters, *Physics of Plasmas* **18**, 062501 (2011).
- [20]. M. Artun and W.M. Tang, *Physics of Plasmas* **1**, 2682 (1994).
- [21]. H. Sugama and W. Horton, *Physics of Plasmas* **5**, 2560 (1998).
- [22]. A.G. Peeters, C. Angioni and D. Strintzi, *Physical Review Letters* **98**, 265003 (2007).
- [23]. G. Tardini et al., *Nuclear Fusion* **49**, 085010 (2009).
- [24]. P. J. Catto and A.N. Simakov, *Physics of Plasmas* **12**, 012501 (2005).
- [25]. S.K. Wong and V.S. Chan, *Physics of Plasmas* **16**, 122507 (2009).
- [26]. F.I. Parra and P.J. Catto, *Plasma Physics and Controlled Fusion* **52**, 045004 (2010).
- [27]. F.I. Parra, M. Barnes and P.J. Catto, submitted to *Nuclear Fusion*. arXiv:1102.4613.
- [28]. M.F.F. Nave et al., submitted to *Plasma Physics and Controlled Fusion* (2011).
- [29]. B.P. Duval et al., *Plasma Physics and Controlled Fusion* **49**, B195 (2007).
- [30]. Y. Camenen et al., *Nuclear Fusion* **51**, 073039 (2011).
- [31]. F. W. Perkins et al., *Physics of Plasmas* **8**, 2181 (2001).
- [32]. L.-G. Eriksson and F. Porcelli, *Nuclear Fusion* **42**, 959 (2002).

- [33]. F.J. Casson et al., *Physics of Plasmas* **16**, 092303 (2009).
- [34]. M. Barnes et al., *Physical Review Letters* **106**, 175004 (2011).
- [35]. E.G. Highcock et al., *Physical Review Letters* **105**, 215003 (2010).
- [36]. E.G. Highcock et al., submitted to *Phys. Plasmas*. arXiv:1105.5750.
- [37]. To give an idea of the complexity of the theoretical problem, we point out that the poloidal velocity will not be counterclockwise at low collisionality, as suggested by Fig.1, but clockwise due to the collisional friction between particles of the type sketched in Fig.1 and a population of trapped particles [17]. Determining the toroidal rotation requires even more work than the poloidal velocity, and the finite-orbit-width effects come in through other mechanisms. For example, the poloidal velocity breaks the up-down symmetry and gives a preferred direction to the turbulent and collisional transport of toroidal angular momentum.
- [38]. The data for TCV was obtained from [10]. In that article, the authors plotted the velocity at the magnetic axis multiplied by I_p against the temperature at the magnetic axis. This is approximately the same as $I_p \Delta V_\pi$ versus ΔT_i because both the rotation and the temperature at the edge are small compared to their values at the magnetic axis.

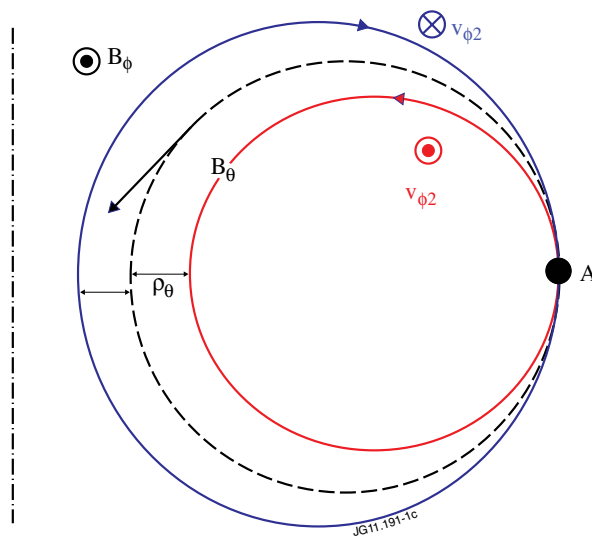


Figure 1: Sketch of drift orbits.

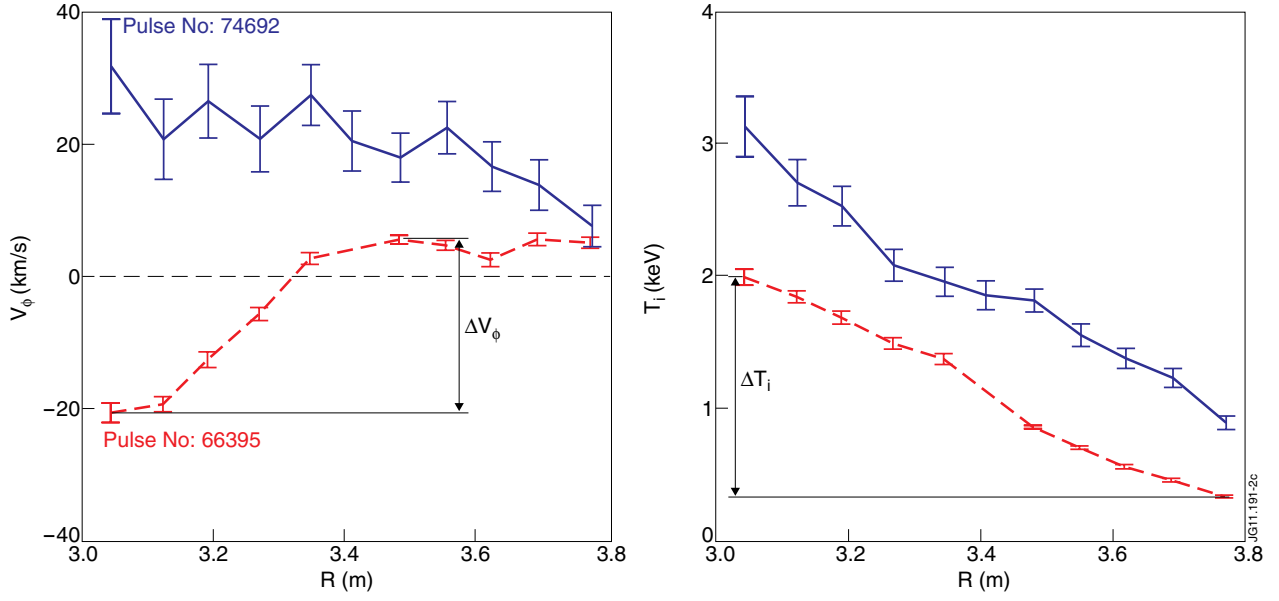


Figure 2: Intrinsic rotation profiles (a) and ion temperature profiles (b) in JET plasmas with ICRH, Pulse No's: 66395 (red) and 74692 (blue). The rotation in the co-current direction is positive rotation. The position of the magnetic axis is around $R = 3m$, the separatrix is around $R = 3.8m$.

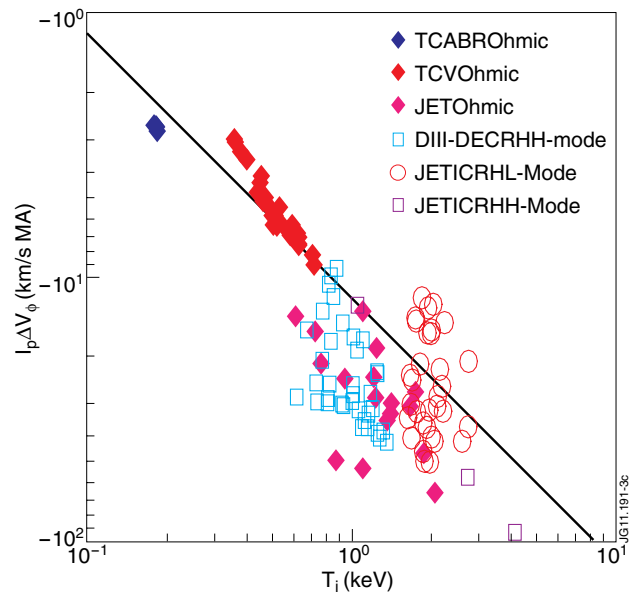


Figure 3: Toroidal velocity difference in the core V multiplied by plasma current I_p against the ion temperature difference T_i in the plasma core. The line is the least-square fit of the data to (4). The slope is $18km \cdot s^{-1} \cdot MA \cdot keV^{-1}$.